DE GRUYTER OPEN

doi: 10.1515/auoc-2016-0008

Ovidius University Annals of Chemistry Volume 27, Number 1, pp. 13-21, 2016

Lipase NS81006 immobilized on Fe_3O_4 magnetic nanoparticles for biodiesel production

Baskar THANGARAJ, Zhaohua JIA, Lingmei DAI, Dehua LIU, Wei DU*

Department of Chemical Engineering, Tsinghua University, Beijing 100084, China

Abstract. Lipase-catalyzed biodiesel production is being the object of extensive research due to the demerits of chemical based catalytic system. Lipase immobilized on Fe_3O_4 magnetic nanoparticles has the integrated advantages of traditional immobilized lipase and free lipase for its rather fast reaction rate and easy separation. It has been demonstrated that free lipase NS81006 has potential in catalyzing the alcoholysis of renewable oils for biodiesel preparation. In this study, Fe_3O_4 magnetic nanoparticles functionalized with organosilane compounds like (3-aminopropyl)triethyloxysilane (APTES) and (3-mercaptopropyl)trimethoxysilane) MPTMS were used as carriers for lipase immobilization. Lipase NS81006 was covalently bound to the organosilane-functionalized magnetic nanoparticles by using glutaraldehyde cross-linking reagent. A biodiesel yield of 89% and 81% could be achieved by lipase immobilized on APTES-Fe_3O_4 and MPTMS-Fe_3O_4 magnetic nanoparticles respectively under optimized conditions of oil to methanol molar ratio 1:3 with three step addition of methanol, reaction temperature 45°C and reaction time duration 12 h. The lipases immobilized on magnetic nanoparticles could be recovered easily by external magnetic field for further use.

Keywords: Fe_3O_4 magnetic nanoparticles, functionalization, immobilized lipase, biocatalysts, transesterification, biodiesel.

1. Introduction

An exhausting fossil fuel resources and increasing environmental degradation have been provoked seriously for alternative fuel [1]. Biodiesel is an alternative energy source which has become a very attractive fuel due to non-toxic, easily biodegradable and their environmental benefits such as lower combustion emissions of carbon monoxide, particulate matter, and sulfur compounds [2]. Biodiesel is alkyl esters of fatty acids which are deriving from plant oils and animal fats. Biodiesel can be produced by transesterification reaction from triglycerides and usually there are two catalytic approaches employed for catalytic transesterification reaction processes such as chemical and biological system. Although chemical based catalytic transesterification process is applied widely on an industrial scale for biodiesel preparation, the process has many demerits such as high energy consumption, challenge in the transesterification reaction of high free fatty acid content triglycerides, separation process like recovery of glycerol and removal of catalyst from the product and the purification of the products [3].

Recently enzymatic transesterification of vegetable oils has appealed more attention due to the advantages of environmental friendliness and effectively converting both triglycerides and FFA (free fatty acids) into FAME (fatty acid methyl esters) [4-6]. There are extensive studies related to immobilized lipase-mediated alcoholysis of vegetable oil for biodiesel production. While in recent years it has been demonstrated that free lipase can efficiently catalyze biodiesel production in oil/water two-phase system. Besides, compared to immobilized lipase, free lipase has several merits like higher reaction rate, lower cost and lower requirements to the feedstock. However, with free lipase as the catalyst for biodiesel production, the recovery, and recycling of the lipase has become one of the major issues for practical application [4]. To integrate the advantages of immobilized lipase and free lipase together, lipase immobilized on magnetic nanoparticles is drawing attention in recent years.

Magnetic nanoparticles are most popular materials due to their high surface to volume ratio for loading a larger amount of lipase, lower mass transfer resistance for reacting with substrates and ease the way of separation from the reaction mixture by external magnetic field [7]. Naked-magnetic nanoparticles are not applicable directly for lipase immobilization and some suitable surface modification or functionalization on the naked-magnetic nanoparticles are necessary before immobilizing lipase onto the nanoparticles [7-9]. It has been found that some organosilane compounds

* Corresponding author: duwei@tsinghua.edu.cn

© 2016 Ovidius University Press

like 3-aminopropyltriethyloxysilane (APTES), *p*-aminophenyltrimethoxysilane (APTS) and mercaptopropyltriethoxysilane (MPTES) can be used as the potential candidates for functionalizing or modifying the surface of the naked magnetic nanoparticles. After modification/functionalization of the magnetic nanoparticles, the lipase can be immobilized onto magnetic nanoparticles either through physical adsorption or covalent interaction [10].

In our previous study [4], it has been found that free lipase NS81006 could efficiently catalyze the transesterification of renewable oils for biodiesel production in a water/oil two phase system. In this paper, exploration on immobilizing lipase NS81006 on magnetic nanoparticles and then applying the immobilized lipase for biodiesel production were carried out for the first time. Firstly, Fe_3O_4 magnetic nanoparticles were synthesized and further functionalized with two organosilanes compounds like APTES and MPTMS. The functionalized magnetic nanoparticles were subsequently adopted for the immobilization of lipase NS81006 through glutaraldehyde coupling reagent. The synthesized magnetic nanoparticles with/without lipases were characterized by FT-IR, XRD, SEM, TEM and VSM techniques. Various factors affecting the lipase immobilization efficiency and lipase activity during immobilization were studied systematically. Further exploration on the immobilized lipase-catalyzed methanolysis for biodiesel preparation was also carried out.

2. Experimental

2.1. Materials

APTES (3-aminopropyltriethoxysilane) and MPTMS (3-mercaptopropyltrimethoxysilane) were purchased from Sigma-Aldrich (St. Louis, MO). Free lipase (NS81006) from the genetically modified *Aspergillus niger* was donated by Novozymes (Denmark). Tributyrin was purchased from Tokyo Chemical Industry, Japan. All the other chemicals were of analytical grade and obtained from local market.

2.2. Characterizations

FT-IR spectroscopic analysis was performed by Thermo Scientific Nicolet iN10 FT-IR Microscope (Thermo Nicolet Corporation, Madison, WI) equipped with a liquid nitrogen cooled MCT detector. Scans of wave number were conducted at 400–4000 cm^{-1}. The crystallinity of the samples was determined by X-ray diffraction (XRD). X-ray diffraction patterns were recorded with XRD-6000 diffractometer (Shimadzu, Japan) using Ni-filtered Cu Kα radiation (λ = 1.54 Å) at 40 kV and 40 mA. Surface morphology of synthesized Fe_3O_4 magnetic nanoparticles was analyzed by using scanning electron microscope (SEM). A Hitachi S-3400N II (Hitachi, Japan) instrument operated at 15 kV was used. Images were obtained at the magnification ranges from 45 × to 30,000× depending on the feature to be traced. TEM measurements were carried out in an FEI TECNAI G2 20 (USA) transmission electron microscope operating at 200 kV. The magnetic properties of the synthesized samples were characterized with a vibrating sample magnetometer (VSM) using IDEASVSM at room temperature.

Biodiesel (fatty acid methyl esters) was analyzed by Agilent 7890AGC (Agilent Technologies, Santa Clara, USA) equipped with CP-FFAPCB capillary column (25m×0.32mm×0.30m, Agilent Technologies, USA). The heptadecanoic acid methyl ester was used as the internal standard. 50 mg of the upper layer and 0.6 mL of 0.7 mg/mL heptadecanoic acid methyl ester (ethanol as a solvent) were mixed thoroughly. The resultant mixture (1 μL) was injected for analysis. The initial column temperature was fixed at 160°C and held for 0.5 min, then heated to 250°C at the rate of 10°C/min and maintained for 6 min. Injector and detector temperatures were assigned to 245°C and 250°C, respectively.

2.3. Preparation of Fe_3O_4 magnetic nanoparticles

Fe_3O_4 magnetic nanoparticles were prepared by co-precipitation method. Iron oxide precursor's materials of $FeSO_4 \cdot 7H_2O$ and $FeCl_3 \cdot 6H_2O$ (molar ratio 1:2) were dissolved in 200 mL deionized water. The mixture was stirred (600 rpm) and heated at 30°C for 30 min, and then 50 mL of ammonia solution (25%) was added dropwise to the mixture. The obtained black precipitated solution was heated at 85°C for 30 min. The resulting Fe_3O_4 magnetic nanoparticles were collected by applying external magnetic field and the particles were washed with deionized water and ethanol. Finally, the resultant magnetic nanoparticles were dried in a hot air oven at 70°C and kept in a desiccator for further use.

2.4. Functionalization of Fe_3O_4 magnetic nanoparticles with APTES and MPTMS as well as glutaraldehyde activation

Fe_3O_4 magnetic nanoparticles (0.5 g) were dispersed in 10 mL of ethanol through ultrasonication for 30 minutes. APTES and MPTMS solutions were added with different amounts (0.05 mL, 0.1 mL, 0.2 mL, 0.3 mL, 0.6 mL, 0.9 mL and 1.2 mL) into the dispersed particles. The mixture was dispersed by ultrasonication sufficiently and then replaced in the shaker for shaking overnight at 25°C.

The obtained functionalized magnetic nanoparticles were collected by external magnetic field and rinsed with deionized water and ethanol to remove the excess organosilane reagents.

Further, the functionalized magnetic nanoparticles were activated by coupling reagent glutaraldehyde. A 20 mL glutaraldehyde solution was

added into the functionalized magnetic nanoparticles. Then, the mixture was shaking at 25°C for 2 h. Finally, the synthesized magnetic nanoparticles were washed well with deionized water to remove the unreacted glutaraldehyde solution. The particles obtained from above mentioned process were applied for lipase immobilization.

2.5. Lipase immobilization

A 10 mL of lipase and phosphate buffer solution (PBS) (pH – 7.0) were added into glutaraldehyde activated magnetic nanocarriers. The mixture was shaken at 25°C for hours. After completion of the reaction, the lipase immobilized on magnetic nanoparticles was washed with PBS solution for several times.

The quantity of lipase bounded on the particles was measured according to the reference [11]. The immobilization efficiency of the lipase was calculated according to the following equation [12],

$$Lipase\ immobilization\ efficiency\ E\ (\%) = = \frac{C_1 - C_0}{C_1} \times 100$$

where E represents lipase immobilization efficiency; C_1 is the amount of the lipase protein existing in solution before immobilization; C_0 is the amount of the lipase protein existing in solution after immobilization.

The immobilized particles were dried and then subject to lipase activity measurement while transesterification reactions were carried out directly without freeze dry.

2.6. Lipase activity assay

The activity of free and immobilized lipase was measured by hydrolysis of tributyrin and the activity recovery was calculated from the following equation [13],

$$Activity\ recovery\ R\ (\%) = \frac{A}{A_0} \times 100$$

where R represents the activity recovery of immobilized lipase, A is the activity of the immobilized lipase, A_0 is the activity of free lipase in solution before immobilization.

2.7. Immobilized lipase-mediated transesterification reaction

Transesterification reactions were carried out in a 100 mL three necked round bottom flask kept in a water bath at 45°C and subject to a mechanical blender with stirring rate of 600 rpm.

The composition of the reactants consisted of 10 mL soybean oil, 0.5 g immobilized lipase and some amount of methanol with stepwise addition of the methanol.

The sample was taken at different time intervals for FAME (fatty acid methyl esters) analysis by gas chromatography.

3. Results and Discussions

3.1. Physical characterization of synthesized naked-Fe_3O_4 and modified Fe_3O_4 magnetic nanoparticles

FT-IR spectra of naked-Fe_3O_4, functionalized Fe_3O_4, lipase immobilized on APTES-Fe_3O_4, lipase immobilized on MPTMS-Fe_3O_4 and pure lipase were presented in Fig. 1 a-f. It could be seen that characteristic absorption bands of the Fe-O stretching vibration ascribed at 559.2 cm^{-1} [14, 15], and the contribution of the absorption at 3400 cm^{-1} was attributed to O-H band [16]. The absorption bands at 1623.1 cm^{-1} [17, 18] and 1396.2 cm^{-1} [8] revealed that the presence of an amino group (N-H) as shown in Fig. 1 a.

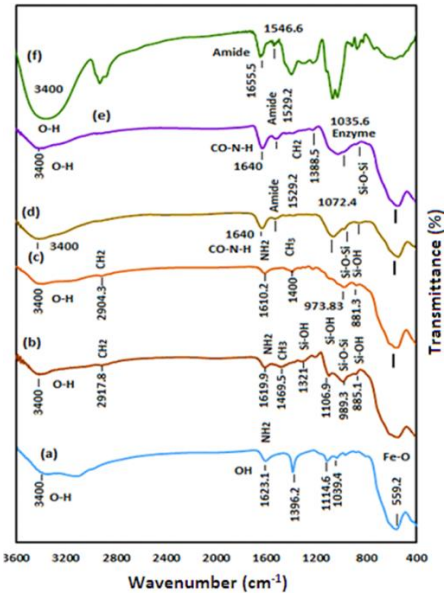

Figure 1. FT-IR spectra of (a) naked-Fe_3O_4 (b) APTES-Fe_3O_4 (c) MPTMS-Fe_3O_4 (d) lipase immobilized on APTES-Fe_3O_4 (e) lipase immobilized on MPTMS-Fe_3O_4 and (f) pure lipase

These results confirmed the synthesis of Fe_3O_4, ammonia solution as a precipitator, which could be functionalized on the surface of the magnetic nanoparticles [18]. The broad band at 1106.9 cm^{-1} and 1321 cm^{-1} were the contribution of silanol group Si-O, and the adsorption bands at 2917.8 cm^{-1} (Fig. 1 b) and 2904.3 cm^{-1} (Fig. 1 c) were the stretching vibration band of CH_2 bonds from APTES molecules [19, 20]. Peaks at 1400 cm^{-1} and 1388.5 cm^{-1} are revealed that in-plane bending vibrations of CH_3 and CH_2 [8]. But the stretching vibration band of CH_2 was disappeared in the lipase immobilized APTES-Fe_3O_4 and MPTES-Fe_3O_4 particles. Fig. 1 c and d were confirmed the lipase immobilized on the particles surface by the variation of other FT-IR spectra.

The lipase immobilized on Fe_3O_4 magnetic nanoparticles clearly showed that the peaks at 1529.2 cm^{-1} and 1640 cm^{-1} are the bending vibration peaks of CO=N-H amide I and amide II variations are represented in Fig. 1 d, e [19, 21]. The pure lipase also have these two bending vibration peaks of amide I and amide II are occurred as shown in Fig. 1 f. Fig. 1 confirmed that the lipase was successfully immobilized on the particles surface.

The crystalline structure of the synthesized naked-Fe_3O_4 and lipases immobilized on APTES-Fe_3O_4 and MPTMS-Fe_3O_4 were characterized by XRD as shown in Fig. 2.

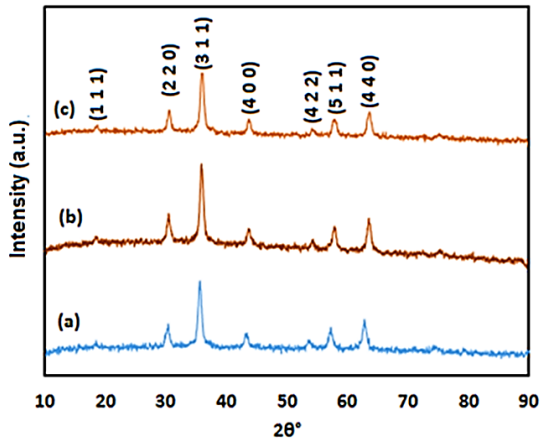

Figure 2. XRD patterns of (a) naked-Fe_3O_4, (b) lipase immobilized on APTES-Fe_3O_4 and (c) lipase immobilized on MPTMS-Fe_3O_4

For the naked-Fe_3O_4 magnetic nanoparticles, diffraction peaks at Bragg angles 2θ ~ 18°, 30°, 35°, 43°, 53°, 57° and 63° were identified, that are corresponded to the crystal planes of (111), (220), (311), (400), (422), (511) and (440) respectively. According to JCPDS card number 19-0629, these obtained peaks were related to Fe_3O_4 with an inverse spinel structure [21, 22].

The XRD patterns revealed that there were no peaks related to impurities. The XRD patterns revealed that lipases immobilized on APTES-Fe_3O_4 and MPTMS-Fe_3O_4 have similar diffraction peaks. The average crystalline size (Cs) of the magnetic nanoparticles was calculated by using the Debye - Scherrer's formula described as follows [23],

$$Crystalline\ size\ (Cs) = \frac{K\,\lambda}{\beta\ cos\theta}$$

where λ is the wavelength of the X-ray wave used, K is the shape factor (0.9), β is the full width at half maximum (FWHM) value of diffraction peak and θ is the angle of diffraction to the peak. The average crystalline size of naked-Fe_3O_4, lipase immobilized on APTES-Fe_3O_4 and MPTMS-Fe_3O_4 magnetic nanoparticles were ~ 20.05 nm, ~ 21.70 nm, and ~21.35 nm.

SEM images of naked Fe_3O_4 magnetic nanoparticles were shown in Fig. 3. SEM images revealed that the particles surface was roughness and the particles get aggregated to a varied extent that might be due to the magnetic dipole moment interaction between the particles [8].

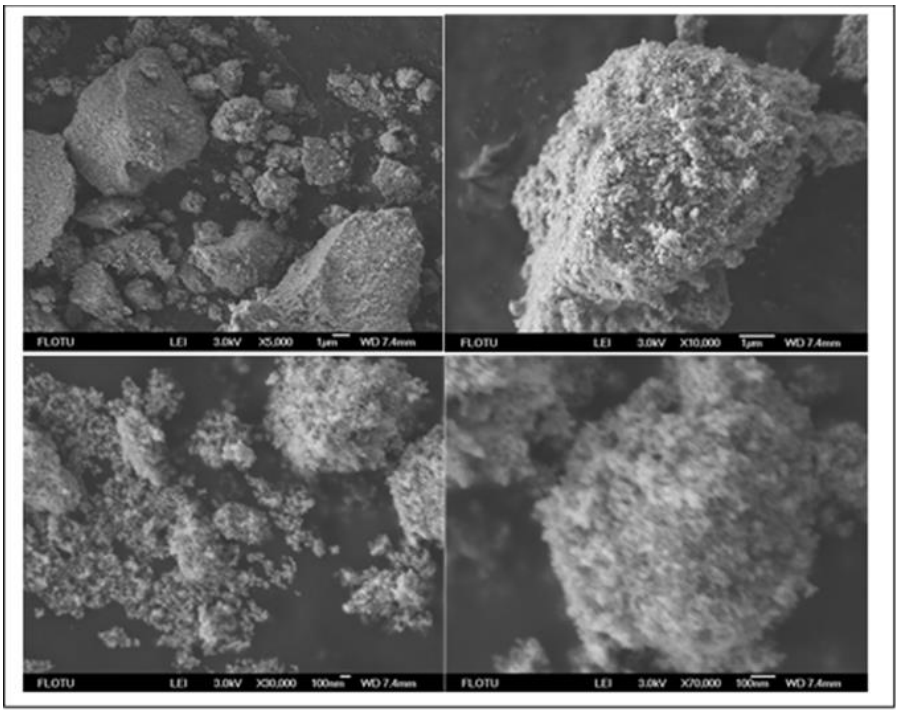

Figure 3. SEM images of naked-Fe_3O_4 magnetic nanoparticles

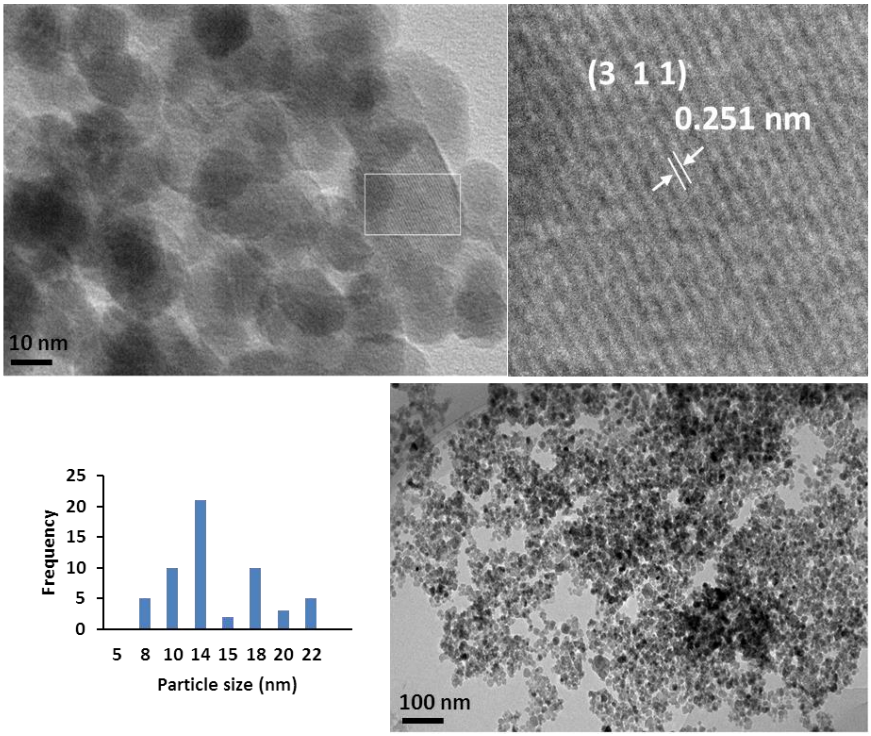

Figure 4. TEM images of naked-Fe_3O_4 magnetic nanoparticles

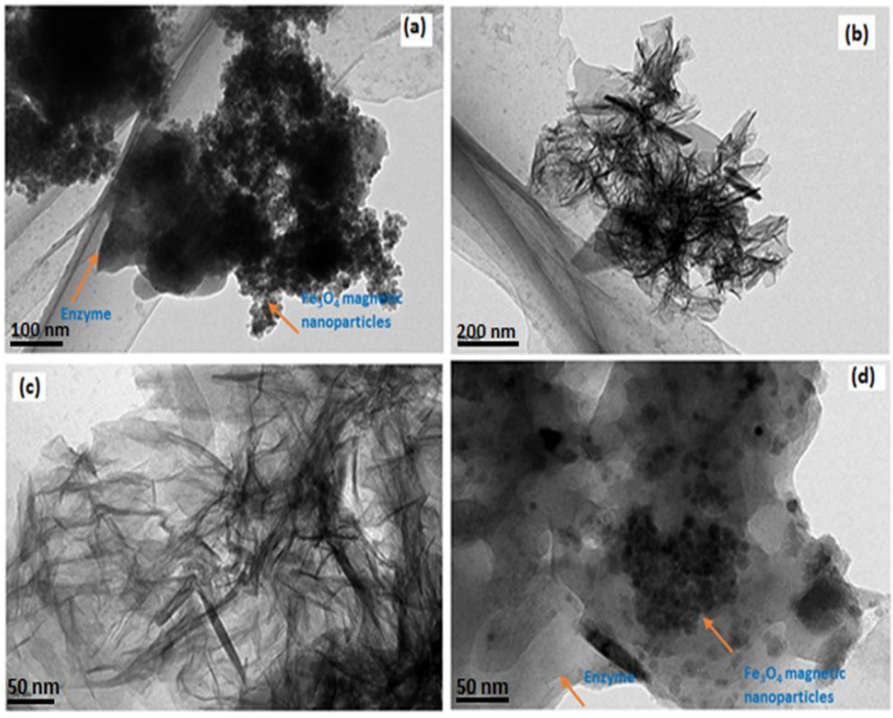

Figure 5. TEM images of (a, b) Lipase immobilized on APTES-Fe_3O_4 and (c, d) MPTMS-Fe_3O_4 magnetic nanoparticles

TEM micrographs of naked-Fe_3O_4 magnetic nanoparticles were represented in Fig. 4. TEM images are also clearly showed that MNPs aggregated and the particle size varied from 10 nm to 20 nm. The particle size and shape were not obtained uniformly due to co-precipitation method used for the preparation of Fe_3O_4 magnetic nanoparticles [24, 25]. The particles have the crystalline plane of (3 1 1) and the *d*- spacing

value calculated between the planes 0.25 nm which corresponded to the dominant diffraction peak of (3 1 1) in XRD pattern as shown in Fig. 2

TEM micrographs of lipase immobilized on Fe_3O_4 magnetic nanoparticles were presented in Fig. 5. These images clearly confirmed that the lipase molecules were bonded on the surface of the magnetic nanoparticles.

The magnetic property of the naked-Fe_3O_4 and lipase immobilized on magnetic nanoparticles was measured at room temperature by vibrating sample magnetometer (VSM) as presented in Fig. 6.

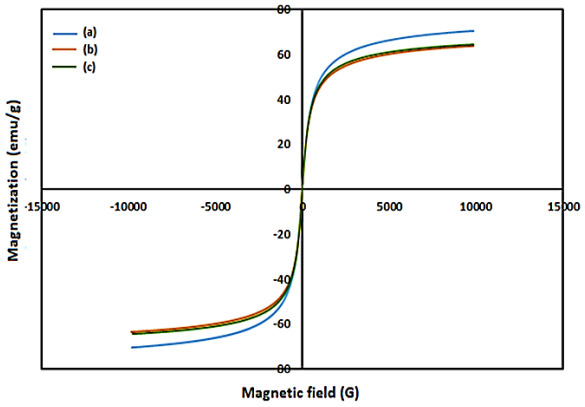

Figure 6. Magnetization vs magnetic field of (a) naked-Fe_3O_4, (b) lipase immobilized on APTES-Fe_3O_4 and (c) lipase immobilized on MPTMS-Fe_3O_4

The saturation magnetization of naked-Fe_3O_4 magnetic nanoparticle was 70.36 emu/g while the saturation magnetization of the lipase immobilized on APTES-Fe_3O_4 and MPTMS-Fe_3O_4 were 63.55 emu/g and 64.37 emu/g respectively. Lipase immobilized on MPTMS-Fe_3O_4 has higher magnetization value than the lipase immobilized on APTES-Fe_3O_4. There was no hysteresis loop in the magnetization curve, indicating these magnetic nanoparticle carrier has superparamagnetic behavior [26]. Herein, these lipases immobilized magnetic nanoparticles could respond to an applied magnetic field and could be recovered easily for further use.

3.2. Factors affecting the immobilization efficiency and activity recovery for lipase immobilization

The factors influencing the lipase immobilization such as the amount of organosilane compound, functionalization time and glutaraldehyde concentration were investigated in the following study.

3.2.1. Effect of organosilane amount. The magnetic nanoparticles were functionalized with different organosilane compounds like (3-aminopropyl)triethoxysilane (APTES) and (3-mercaptopropyl)trimethoxysilane (MPTMS). The amount of silane compound was varied, such as 0.05 mL, 0.1 mL, 0.2 mL, 0.3 mL, 0.6 mL, 0.9 mL and 1.2 mL. The immobilization efficiency and activity recovery results were presented in Fig. 7. The maximum lipase immobilization efficiency and activity recovery were obtained like 98.8% and 81.8% respectively. It was also found that the magnetic nanoparticles functionalized with APTES had higher activity recovery than that of functionalized with MPTMS.

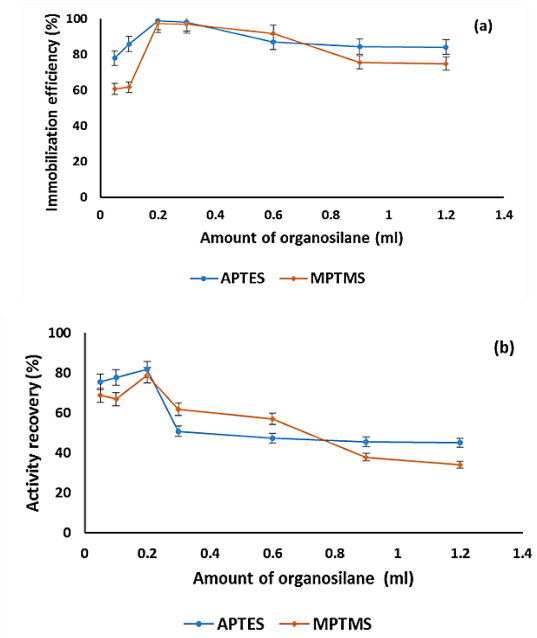

Figure 7. Effect of amount of organosilane on (a) the immobilization efficiency and (b) activity recovery.

*Lipase immobilization conditions: functionalization time 12 h, lipase amount 1 mL, reaction temperature 25°C, glutaraldehyde concentration 10%, immobilization time 6h.

3.2.2. Effect of functionalization time. Functionalization time is playing an important role in lipase immobilization. From Fig. 8, it could be seen that the immobilization efficiency of 96.4% could be obtained by APTES at 1 h while the highest immobilization efficiency achieved by MPTMS at 3h.

3.2.3. Effect of glutaraldehyde concentration. The silane functionalized magnetic nanoparticles were further connected to aldehyde groups by using glutaraldehyde coupling reagent to create a covalent bond formation with the lipase molecules.

The effect of glutaraldehyde concentration on the immobilization efficiency and the activity recovery of the immobilized lipase are shown in Fig. 9. The highest immobilization efficiency and activity recovery were obtained by 10% (v/v) glutaraldehyde. Glutaraldehyde concentration is less than 10% (v/v) answered in deficient activation of the functionalized magnetic nanoparticles, while higher concentrations affected excessive coupling reagent of glutaraldehyde, which might be a steric effect for

lipase. Due to steric hindrance effect, the activity of the immobilized lipase ebbing [27].

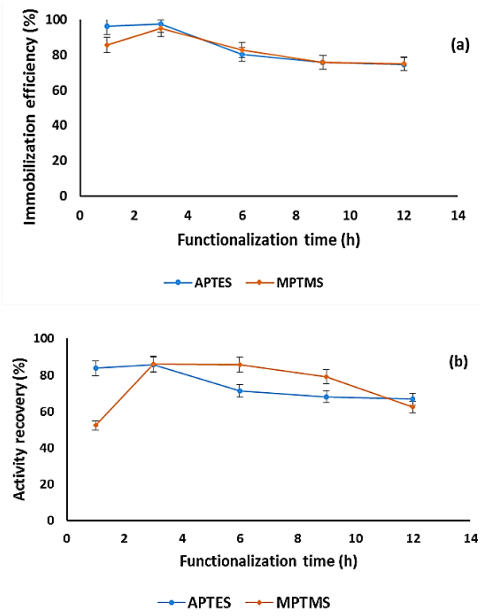

Figure 8. Effect of functionalization time on (a) the immobilization efficiency and (b) activity recovery

*Lipase immobilization conditions: APTES and MPTMS 0.2 ml, lipase amount 1 mL, glutaraldehyde concentration 10%, reaction temperature 25°C, immobilization time 6 h.

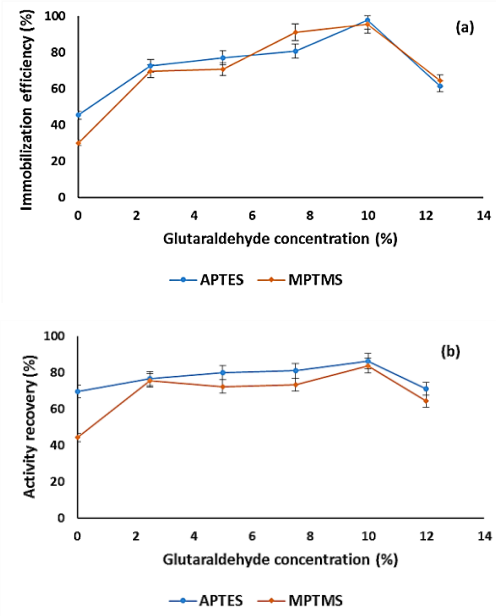

Figure 9. Effect of glutaraldehyde concentration on (a) the immobilization efficiency and (b) activity recovery.

*Lipase immobilization conditions: APTES and MPTMS 0.2 mL, functionalization time 3 h, lipase amount 1 mL, reaction temperature 25°C, immobilization time 6 h.

Xie *et al* achieved the maximum immobilization efficiency and activity recovery like above 80% and 65% at 10% glutaraldehyde concentration by lipase (Lipozyme-TL) immobilized on APTES-Fe_3O_4 [5]. This study achieved the maximum immobilization efficiency and activity recovery were obtained 97% and 86% at same concentration of glutaraldehyde by lipase (NS81006) immobilized on APTES-Fe_3O_4 while lipase immobilized on MPTMS-Fe_3O_4 also attained maximum immobilization efficiency and activity recovery. The optimum concentration of glutaraldehyde was found 10% for both organosilane compounds.

3.3. Immobilized lipase catalyzed transesterification for biodiesel production

The lipase immobilized on magnetic nanoparticles was further used for biodiesel production and the factors are influencing the methanolysis reaction were investigated in the following study.

3.3.1. Effect of reaction temperature. The effect of reaction temperature was examined by lipase immobilized catalysts at various temperature ranges from 40°C to 55°C as shown in Fig. 10.

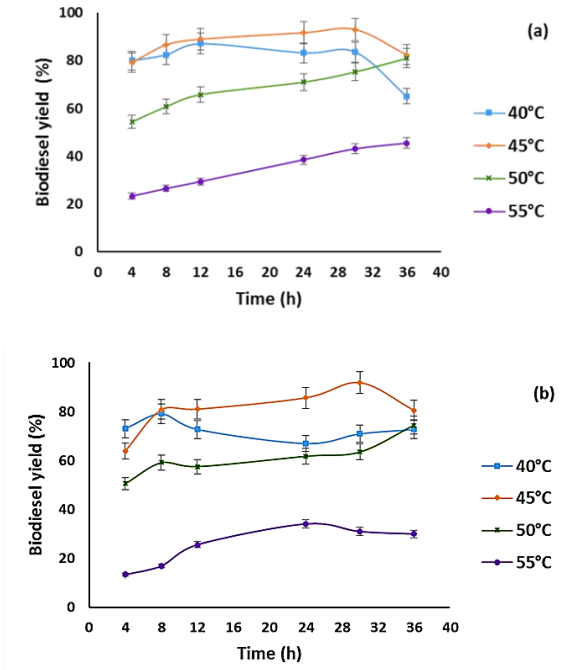

Figure 10. Effect of reaction temperature on the lipase immobilized on (a) APTES-Fe_3O_4 and (b) MPTMS-Fe_3O_4 catalyzed biodiesel production.

*Reaction conditions: soybean oil 10 mL, lipase immobilized catalyst 0.5 g, oil to methanol molar ratio 1:3, three steps addition of methanol, stirring rate 600 rpm.

The highest biodiesel yield was achieved at 45°C. The biodiesel yield reduced at higher reaction temperatures like 50°C and 55°C which might be due to inactivation of lipase [28]. Lipase immobilized on

APTES-Fe_3O_4 gave better catalytic activity than that immobilized on MPTMS-Fe_3O_4.

3.3.2. Effect of oil to methanol molar ratio. Oil to methanol molar ratio is one of the most important factor affecting the yield of biodiesel. Herein, the various molar ratio of oil to methanol was carried out such as 1:3, 1:6, 1:8 and 1:10 with three stepwise addition of methanol and the related results as presented in Fig. 11. The highest biodiesel yield could be attained at 1:3 molar ratio. Lipase immobilized on APTES-Fe_3O_4 and MPTMS-Fe_3O_4 had better yield at lower ratios like 1:3 and 1:6, while the other higher ratios like 1:8 and 1:10 decreased the biodiesel yield. An excessive amount of methanol could be reduced the activity of immobilized lipase in the reaction system. Lipase immobilized on APTES-Fe_3O_4 and MPTMS-Fe_3O_4 could be achieved biodiesel yield like 89% and 81% under the optimum conditions such oil to methanol molar ratio 1:3 with three stepwise addition of methanol, reaction temperature 45°C and reaction time 12 h respectively.

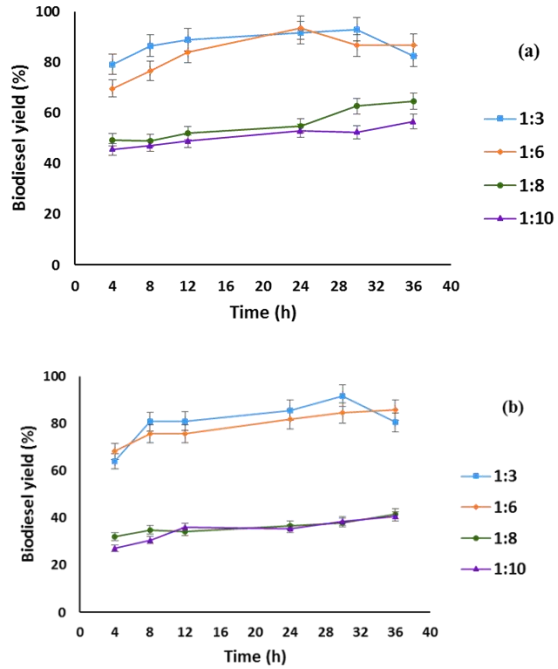

Figure 11. Effect of oil to methanol molar ratio on the lipase immobilized on (a) APTES-Fe_3O_4 and (b) MPTMS-Fe_3O_4 catalyzed biodiesel production.

*Reaction conditions: soybean oil 10 mL, lipase immobilized catalyst 0.5 g, temperature 45°C, three steps addition of methanol, stirring rate 600 rpm.

There are several other immobilized lipases, which are also reported in the literature. Xie *et al.* achieved the highest biodiesel yield above 90% by lipase immobilized on APTES-Fe_3O_4 under the optimum conditions [5]. Yagiz *et al.* achieved the biodiesel yield of 92.8% by lipozyme TL IM immobilized on hydrotalcite [29]. A high soybean oil conversion achieved 87% at 30 h under optimum reaction conditions by lipase immobilized on magnetic chitosan microspheres [10]. Dizge and Keskinler achieved the biodiesel yield 90% from canola oil by using immobilized lipase *Thermomyces lanuginosus* [30]. The maximum biodiesel was obtained 93% at 25°C in 24 h under the optimized reaction conditions by *Thermomyces lanuginosus* lipase immobilized onto olive pomace and retained its activity up to 10 repeated batches [31].

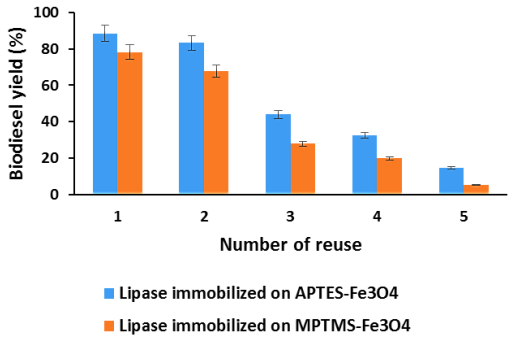

Figure 12. Catalyst reusability of immobilized lipase by transesterification reaction.

*Reaction conditions: soybean oil 10 mL, lipase immobilized catalyst 0.5 g, oil to methanol molar ratio 1:3, three steps addition of methanol, temperature 45°C, time 12 h, stirring rate 600 rpm.

The immobilized lipase was recovered by strong magnetic field and then reused for a new transesterification reaction. It was noticed that immobilized lipase loses their activity gradually during the repeated uses as shown in Fig. 12, which might be due to the leakage of lipase caused by mechanically blender system. Other forms of bioreactor can be explored in the future study to avoid such loss during the repeated uses [29, 32]. Xie *et al.* reported that the stability of immobilized lipase, the conversion was significantly reduced at every cycle. The loss of activity may accredited to conformational changes of lipase or to methanol deactivation of lipase during the reaction procedure [10].

4. Conclusions

Lipase NS81006 was successfully immobilized onto APTES and MPTMS functionalized magnetic nanoparticles. The TEM and XRD characterizations revealed that the magnetic nanoparticles have crystalline nature and the particle sizes were around 20 nm. In terms of activity recovery and biodiesel yield, lipase immobilized on APTES-Fe_3O_4 magnetic nanoparticles gave better results than that of lipase immobilized on MPTMS-Fe_3O_4 magnetic nanoparticles. A biodiesel yield of 89% and 81% could be achieved by lipase immobilized on APTES-Fe_3O_4 and MPTMS-Fe_3O_4 magnetic nanoparticles

respectively. The lipases immobilized on magnetic nanoparticles could be recovered easily for further use and had a great prospect for biodiesel production.

Acknowledgements

The authors express their gratitude to the support from Science & Technology Department of Guangdong Province (2015B020215001) and National Natural Science Foundation of China (21376139).

References

[1] B. Thangaraj, P.R. Samuel, Int. J. Sustainable Energy **33**, 525 (2013).
[2] D.S. Martino, R. Tesser, L. Pengmei, E. Santacesaria, Energy Fuels **22**, 207 (2008).
[3] A. Bajaj P. Lohan, P.N. Jha, R. Mehrotra, J. Mol. Catal. B: Enzym. **62**, 9 (2010).
[4] Y. Li, W. Du, D. Liu, J. Mol. Catal. B: Enzym. **102**, 88 (2014).
[5] W. Xie, N. Ma, Energy Fuels **23**, 1347 (2009).
[6] R. Luque, J.H. Clark, ChemCatChem **3**, 594 (2011).
[7] P.A. Johnson, H.J. Park, A.J. Driscoll, Methods Mol. Biol. **679**, 183 (2011).
[8] J. Wang, G. Meng, K. Tao, M. Feng, X. Zhao, Z. Li, H. Xu, D. Xia, PLOS ONE **7**, 1 (2012).
[9] W. Wu, Q. He, C. Jiang, Nanoscale Res. Lett. **11**, 397 (2008).
[10] W. Xie, J. Wang, Biomass Bioenergy **36**, 373 (2012).
[11] M.M. Bradford, Anal. Biochem.**72**, 248(1976).
[12] B. Hu, J. Pan, H.L. Yu, J.W Liu, J.H. Xu, Process Biochem. **44**, 1019 (2009).
[13] J. Huang, Y. Liu, X. Wang, J. Mol. Catal. B: Enzym. **55**, 49 (2008).
[14] K. Can, M. Ozmen, M. Ersoz, Colloids Surf. B **71**, 154 (2009).
[15] L. Chen, Z. Lin, C. Zhao, Y. Zheng, Y. Zhou, H.J. Peng, J. Alloys Compd. **509**, L1 (2011).
[16] S. Taira, D. Kaneko, K. Onuma, A. Miyazato, T. Hiroki, Y.K. Konishi, Y. Ichiyanagi, Inter.J. Inorg. Chem. **2012**, 1 (2012).
[17] X.C. Shen, X.Z. Fang, Y.H. Zhou, H. Liang, Chem. Lett. **33**, 1468 (2004).
[18] X. Wang, P. Dou, P. Zhao, C. Zhao, Y. Ding, P. Xu, ChemSusChem **2**, 947(2009).
[19] Z. Bo, X. J. Min, L.Y. Qi, L.H. Zhou, Sci. China. Ser. B-Chem. **51**, 145 (2008).
[20] Y. Jiang, L. Shi, Y. Huang, J. Gao, X. Zhang, L. Zhou, ACS Appl. Mater. Interfaces **6**, 2622 (2014).
[21] A. Jafari, M. Salouti, S.F. Shayesteh, Z. Heidari, A.H. Rajabi, K. Boustani, A. Nahardani, Nanotechnology **26**, 1 (2015).
[22] J. Hong, D. Xu, J. Yu, P. Gong, H. Ma, S. Yao, Nanotechnology **18**, 1 (2007).
[23] Y. Yao, S. Miao, S. Yu, L.P. Ma, H. Sun, S. Wang, J. Colloid Interface Sci. **379**, 20 (2012).
[24] S. Laurent, D. Forge, M. Port, A. Roch, C. Robic, L.V. Elst, R.N. Muller, Chem. Rev. **108**, 2064 (2008).
[25] A.H. Lu, E.L. Salabas, F. Schuth, Angew. Chem. Int. Ed. **46**, 1222 (2007)
[26] J. Zhu, B. Zhang, J. Tian, J. Wang, Y. Chong, X. Wang, Y. Deng, M. Tang, Y. Li, C. Ge, Y. Pan, H. Gu, Nanoscale **7**, 3392 (2015).
[27] Liu, X.; Guan, Y.; Shen, R.; Liu, H. J. Chromat. **1-2**, 91 (2005).
[28] C.Y. Yu, L.Y. Huang, I.C. Kuan, S.L. Lee, Int. J. Mol. Sci. **14**, 24074 (2013).
[29] F. Yagiz, D. Kazan, A.N. Akin, Chem. Eng. J. **134**, 262 (2007).
[30] T.P.N. Ngo, A. Li, K.W. Tiew, Z. Li, Bioresour. Technol. **145**, 233 (2013).
[31] N. Dizge, B. Keskinler, Biomass Bioenergy **32**, 1274 (2008).
[32] Y. Yücel, Bioresour. Technol. **102**, 3977 (2011).

Received: 07.05.2016
Received in revised form: 20.05.2016
Accepted: 23.05.2016